

**Distillable entanglement and area laws in spin and harmonic-oscillator systems**Daniel Cavalcanti,<sup>1</sup> Alessandro Ferraro,<sup>1</sup> Artur García-Saez,<sup>1</sup> and Antonio Acín<sup>1,2</sup><sup>1</sup>*ICFO-Institut de Ciències Fòniques, Mediterranean Technology Park, 08860 Castelldefels (Barcelona), Spain*<sup>2</sup>*ICREA-Institució Catalana de Recerca i Estudis Avançats, Lluís Companys 23, 08010 Barcelona, Spain*

(Received 7 May 2008; published 18 July 2008)

We address the presence of nondistillable (bound) entanglement in natural many-body systems. In particular, we consider standard harmonic and spin- $\frac{1}{2}$  chains, at thermal equilibrium and characterized by few interaction parameters. The existence of bound entanglement is addressed by calculating explicitly the negativity of entanglement for different partitions. This allows us to individuate a range of temperatures for which no entanglement can be distilled by means of local operations, despite the system being globally entangled. We discuss how the appearance of bound entanglement can be linked to entanglement-area laws, typical of these systems. Various types of interactions are explored, showing that the presence of bound entanglement is an intrinsic feature of these systems. In the harmonic case, we analytically prove that thermal bound entanglement persists for systems composed by an arbitrary number of particles. Our results strongly suggest the existence of bound entangled states in the macroscopic limit also for spin- $\frac{1}{2}$  systems.

DOI: [10.1103/PhysRevA.78.012335](https://doi.org/10.1103/PhysRevA.78.012335)

PACS number(s): 03.67.Mn

**I. INTRODUCTION**

An ubiquitous scenario in quantum information science consists of two (or more) parties sharing entangled quantum states and performing operations on them. Ideally the shared states are pure and maximally entangled. However, this is hardly the case in practice. As a matter of fact, the available states are always mixed, due to unavoidable errors in the preparation stage or noise in the considered process. Entanglement is also very fragile in this sense, and this is certainly the main obstacle to actual applications of quantum information ideas.

Entanglement distillation plays an important role to correct the degradation of entanglement in real situations [1,2]. It consists of the application of local operations supplied by classical communication (LOCC) that allow the parties to extract maximally entangled states out of a bunch of mixed states. Unfortunately not all entangled states are distillable [3]. There are states  $\rho$  from which no LOCC strategy is able to extract pure-state entanglement, even if many copies of  $\rho$  are available. These states are known as *bound entangled*.

The existence of bound entangled states was proven in [3] by noting that any quantum state with a positive partial transposition (PPT) [4] is nondistillable. Since there were already examples of PPT entangled states [5], the connection between nondistillability and the positivity of partial transposition automatically led to the first examples of bound entangled states. Later, strong evidence was provided for the existence of bound entangled states with nonpositive partial transposition (NPPT) [6]. Independently of partial transposition, bound entangled states have a clear operational definition: an entangled state of  $n$  parties is bound entangled whenever the  $n$  parties cannot distill any pure-state entanglement out of it by LOCC. Although several examples of bound entangled states have appeared so far [7], simple recipes to construct such kind of states are still lacking. It is thus not completely clear whether bound entanglement is basically a mathematical artifact or it “naturally” appears in physically relevant quantum systems. The main motivation of this work

goes precisely along this direction, since we study whether bound entanglement is present in standard many-body quantum systems. By this, we mean systems (i) characterized by a few interaction parameters, (ii) in thermal equilibrium with their environment, (iii) consisting of a macroscopic number of particles.

Very recently a few works have also addressed this question. In Ref. [8] bound entanglement was detected in the thermal state of spin systems, consisting of up to nine spins. More recently, three-qubit bound entangled states were obtained as the reduced state of the XY model in the thermodynamical limit [9]. In a previous contribution we have considered the problem of finding bound entangled thermal states in some specific system consisting of a macroscopic number of harmonic oscillators [10]. The main goal of the present paper is to give a detailed description of these results and extend them to other systems. Specifically, we directly calculate the entanglement in different partitions of thermal states for harmonic oscillators and spin systems and identify a temperature range for which bound entanglement is present. In the harmonic case with nearest-neighbor interaction, we first consider systems composed of hundreds of particles and then explicitly prove that bound entanglement indeed persists in the macroscopic limit, i.e., when  $n \rightarrow \infty$ . Moreover, we offer an explanation of the results in terms of the entanglement area law, a property satisfied by standard many-body systems [11,12]. Due to the general validity of area laws, we see that the presence of bound entanglement is a common feature of these systems. We explicitly analyze a variety of different systems, ranging from critical to noncritical situations and to spin chains characterized by a complex behavior of the entanglement in the ground state. In all these cases we see that there is a range of temperatures for which no entanglement can be distilled by means of LOCC, despite the system being globally entangled.

The paper is organized as follows. In the next section we introduce the main intuition that elucidates the emergence of bound entanglement in thermal states, recalling briefly some known results about entanglement-area laws. Then, in Sec. III we present the analysis of harmonic systems. In particu-

lar, in Sec. III B numerical results regarding finite size systems are presented, whereas in Sec. III C we give the analytical calculations in the macroscopic limit for systems with nearest-neighbor interactions. In Sec. IV, we show that similar results can also be obtained for spin systems, even if in this case, and due to numerical limitations, systems composed only by a small number of particles have been considered. We close the paper with some concluding remarks in Sec. V.

## II. MULTIPARTITE BOUND ENTANGLEMENT AND AREA LAWS

Let us present the main intuition behind our construction of bound entangled thermal states. Consider a quantum system of  $n$  particles described by a local Hamiltonian. For the sake of simplicity, in what follows we restrict our analysis to one-dimensional systems of  $n$  particles. A common property of these systems is that the ground-state entanglement obeys an area law. This means that the entanglement of a bipartite splitting of the system into two groups scales at most as the number of connections between the groups (i.e., the area which separates them). We recall that the entanglement for a bipartite splitting of pure states is uniquely quantified by the entropy of one of the subsystems [13,14]. In general, this quantity scales as the volume of the subsystem, and not as its boundary, for an arbitrary state belonging to the whole Hilbert space of the  $n$  particles. However, as said, this is not the case for the great majority of ground states of local Hamiltonian systems.

Entanglement-area relations were first recognized in connection with the physics of black holes, for which the Von Neumann entropy scales as the surface at the event horizon [15]. In recent years, the advances of entanglement theory allowed for the exploration of this behavior also for a variety of systems typical of condensed matter physics (see Ref. [11] and references therein). Remarkably, many analytical results have been found for harmonic systems for which concepts from the theory of Gaussian quantum states can be applied. As an example, a strict entanglement-area relation has been established for noncritical one-dimensional systems with finite range interaction, while logarithmic corrections appear in the critical case [16–18]. In particular, the entanglement, as measured by the log negativity [19], has been proven to scale proportionally to the area. Similar behaviors have also been found for spin systems. Concerning thermal states, it has recently been demonstrated that the total amount of correlations (measured by the mutual information) in a bipartite split scale at most as the area [20]. This, in turn, gives an upper bound to the entanglement.

Consider now a translationally invariant system composed by an even number  $n$  of particles (labeled from 1 to  $n$ ). Let us focus our attention on two different partitions of it, one in which a contiguous half of the particles belongs to group  $A$  and the other half to  $B$  (we will refer to such kind of partition as half-half), and another partition in which the particles with even label belong to  $A$  and the rest to  $B$  (even-odd partition). Because of the area law, the entanglement saturates for sufficiently large  $n$  for the half-half partition, while it increases

with  $n$  for the even-odd partition. In this configuration, it is reasonable to expect that, by increasing the temperature, the entanglement in the even-odd partition is more robust to thermal noise than in the half-half partition, and that this behavior is preserved for large systems. Denote by  $T_{\text{th}}^{h:h}$  ( $T_{\text{th}}^{e:o}$ ) the threshold temperatures at which the partial transposition with respect to all half-half (even-odd) partitions becomes positive [21]. Because of the area law, one can expect that  $T_{\text{th}}^{h:h}$  is strictly smaller than  $T_{\text{th}}^{e:o}$ . Thus there emerges a range of temperatures for which the system is still entangled (as detected by the entanglement in the even-odd partition), nevertheless, single particles cannot distill pure entanglement (as the half-half partitions become PPT). This is because, for any pair of particles, there is always a half-half partition for which they are in opposite sides and the partial transposition is positive according to this splitting (remember that this is a sufficient condition for nondistillability [3]). In other words, bound entangled states are expected to appear under these conditions. The rest of the paper is devoted to verify and put on solid ground this intuition for various relevant examples of many-body systems.

Before proceeding, let us relate our finding to two related works studying the presence of bound entanglement in systems with local interactions. First, in Ref. [8] the existence of thermal entangled states which are PPT with respect to any bipartition was proven for systems consisting of up to nine spins. For such states, distillation of pure-state entanglement is impossible even if the parties arbitrarily combine together. As said above, we will instead show the existence of bound entangled states only with respect to fully local distillation procedures but for an arbitrary number of particles. Actually, for the harmonic systems considered here we explicitly prove that no entangled states PPT with respect to any bipartition exists. Second, in Ref. [9], the authors find bound entanglement in the reduced three-qubit state of a macroscopic system. Here, we focus on the existence of bound entanglement in the whole thermal state of the system.

## III. HARMONIC OSCILLATORS

In this section, we first introduce the harmonic systems that we are going to consider in order to test the ideas exposed above. Then, in Sec. III B, we perform numerical calculations for different types of interactions in systems of finite size. In Sec. III C, analytical results are presented for the significant case of nearest-neighbor interaction in the macroscopic limit.

### A. The systems

Consider a system composed of  $n$  harmonic oscillators, each one associated with position and momentum operators  $x_i$  and  $p_i$ , respectively ( $i=1, \dots, n$ ), described by the Hamiltonian [22]

$$H = \frac{1}{2} \left( \sum_i p_i^2 + \sum_{i,j} x_i V_{i,j} x_j \right). \quad (1)$$

The diagonal elements of the matrix  $V$  describe the on-site interaction, while the nondiagonal terms give the coupling

between oscillators  $i$  and  $j$ . Note that this Hamiltonian is quadratic in the canonical coordinates and the oscillators are coupled through their position degrees of freedom. In this scenario both the ground and the thermal states turn out to be Gaussian, so they are completely described by their covariance matrix  $\gamma$ . Introducing the vector  $S = (x_1, \dots, x_n, p_1, \dots, p_n)$ , the latter is defined as follows:

$$\gamma_{kl} = \text{Re}(\text{Tr}\{\varrho[S_k - \bar{S}_k][S_l - \bar{S}_l]\}), \quad (2)$$

where  $\varrho$  denotes the density matrix of the state and  $\bar{S}_k = \text{Tr}(\varrho S_k)$ . Considering the thermal state  $\varrho = \exp[-H/T]/\text{Tr}\{\exp[-H/T]\}$  at temperature  $T$ , the corresponding covariance matrix is given by [23]

$$\gamma(T) = [V^{-1/2}W(T)] \oplus [V^{1/2}W(T)], \quad (3)$$

where

$$W(T) = \mathbb{1}_n + 2[\exp(V^{1/2}/T) - \mathbb{1}_n]^{-1} \quad (4)$$

and  $\mathbb{1}_n$  denotes the  $n \times n$  identity matrix. In the ground-state case  $W(0)$  is given by the identity matrix and thus  $\gamma(0) = V^{-1/2} \oplus V^{1/2}$ .

The entanglement properties of the ground and thermal states corresponding to Hamiltonian (1) were first studied by Audenaert *et al.* [23]. There, an analytical expression for the entanglement (quantified by the log negativity [19]) between two complementary groups of oscillators,  $A$  and  $B$ , was given in terms of the covariance matrix of the state, which can be written, in turn, only in terms of the matrix  $V$ . Then one gets the general formula for the log negativity of a thermal state at temperature  $T$ :

$$E_l = \sum_{k=0}^{n-1} \log_2\{\max[1, \lambda_k(Q)]\}, \quad (5)$$

where  $Q = P\omega^{-1}P\omega^+$  and  $\omega^\pm = W(T)^{-1}V^\pm \frac{1}{2}$ . We denoted by  $\{\lambda_k[Q]\}_{k=0}^{n-1}$  the spectrum of the matrix  $Q$ , whereas  $P$  is an  $n \times n$  diagonal matrix with the  $i$ th entry given by 1 or  $-1$  depending on which group,  $A$  or  $B$ , oscillator  $i$  belongs to. This study was later extended in Ref. [16] where an area law for ground-state entanglement was proven. As far as for thermal states, an upper bound for the entanglement in terms of the number of connecting points in a given bipartition was also established [18], but the lack of a lower bound limits us to get a strict area law in this case.

In the case of a harmonic chain with nearest-neighbor interactions and periodic boundary conditions, the system is described by the Hamiltonian (1) with a circulant potential matrix  $V$  given by

$$V^n = C(1, -c, 0, \dots, 0, -c). \quad (6)$$

Where  $C$  denotes a circulant matrix. The system is defined for  $0 \leq c < 1/2$  and it is equivalent to a chain of harmonic oscillators coupled with a springlike interaction. A variety of physical systems can be modeled by such interaction, going from vibrational degrees of freedom in crystal lattices and ion traps to free scalar Klein-Gordon field. We recall that its ground-state entanglement exhibits a critical behavior when  $c \rightarrow 1/2$  [16,24,25].

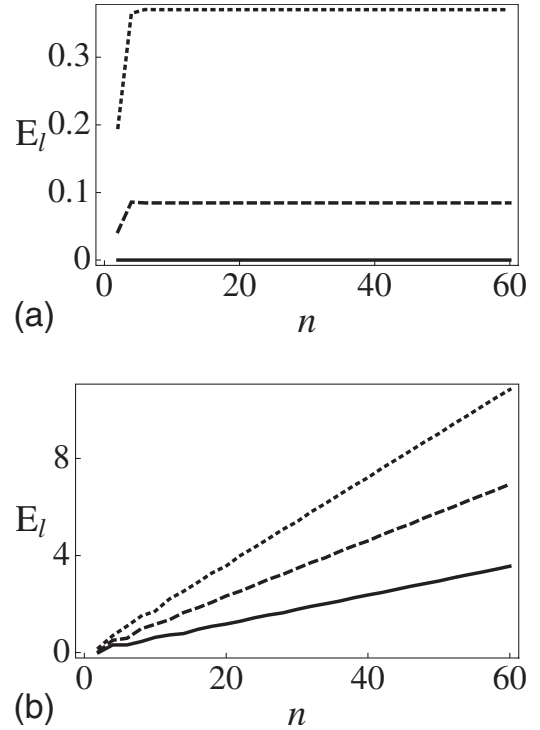


FIG. 1. Log negativity  $E_l$  as a function of the number of oscillators  $n$  for half-half (a) and the even-odd (b) partitions. Temperatures are  $T=0.45$  (solid line),  $T=0.4$  (dashed line), and  $T=0.35$  (dotted line), and  $c=0.4$  (the same behavior is found for other values of  $c$ ). For  $T=0.45$  the state is bound entangled.

In order to test the general validity of the connection between bound entanglement and area laws mentioned in Sec. II, we have also considered other systems. As an example we will report here some results concerning the *next-to-nearest interaction* defined by the potential matrix [17]

$$V^{nn} = C(2 + 4\mu^2, -4\mu, 1, 0, \dots, 0, 1, -4\mu). \quad (7)$$

This system has been shown to be critical (gapless) and to violate the area law for  $0 < \mu < 1$  in the ground state. Nevertheless, as already mentioned, no violation of the area law is possible for nonzero temperatures in view of the results in Ref. [20].

## B. Numerical results

Let us first consider the nearest-neighbor interaction given by Eq. (6). We used Eq. (5) to compute the log negativity for the even-odd and the half-half partitions [21] for different temperatures and number of particles. As already recalled, in Ref. [23] it is shown that a strict area law holds for this system in the ground state. Actually, our calculations show that the log negativity follows a strict area law for nonzero temperatures as well. We depicted in Fig. 1 the log negativity as a function of the number of particles, for fixed coupling and different temperatures. One can clearly see that, apart from a transient for small  $n$ , the log negativity increases linearly with  $n$  for the even-odd case, while it saturates for the half-half partition. Furthermore, the change of the system temperature just affects the rate at which entanglement in-

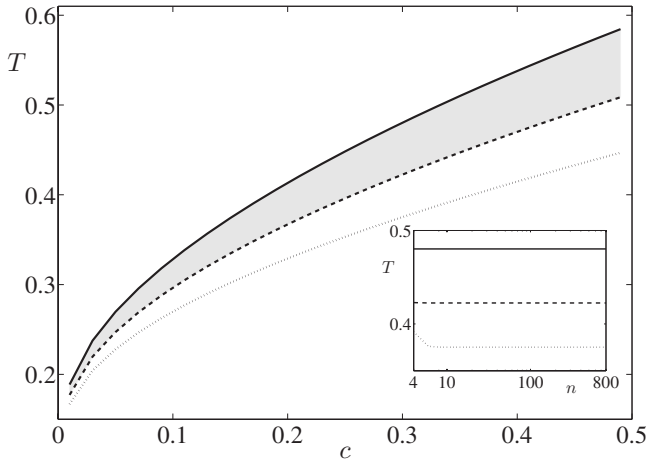


FIG. 2. Threshold temperatures above which the log negativity is zero in the even-odd ( $T_{\text{th}}^{e:o}$ , solid line) and half-half ( $T_{\text{th}}^{h:h}$ , dotted line) partitions. The thresholds are plotted as a function of the coupling constant  $c$  for the Harmonic chain with nearest-neighbor interactions composed by 800 oscillators. The intermediate line (dashed) shows the temperature  $T_{\text{th}}^{1:n-1}$  above which the state is separable in all the partitions  $1:n-1$ . Inset:  $T_{\text{th}}^{e:o}$  (solid line),  $T_{\text{th}}^{h:h}$  (dotted line), and  $T_{\text{th}}^{1:n-1}$  (dashed line) as a function of the number  $n$  of oscillators composing the system (log-lin scale). The oscillators interact via nearest-neighbor couplings with  $c=0.3$  (the same behavior is found for other values of  $c$ ). The gap  $T_{\text{th}}^{e:o} - T_{\text{th}}^{h:h}$  is seen to remain constant with the size of the system, apart from an initial transient.

creases with  $n$  for the even-odd partition and the entanglement saturation value for the half-half partition. The validity of a strict area law has then a remarkable consequence: being the log negativity dependence on  $n$  the same (linear or constant) for all  $T$ , then  $E_f$  goes to zero as  $T$  increases independently of  $n$ . In other words, the threshold temperatures  $T_{\text{th}}^{h:h}$  and  $T_{\text{th}}^{e:o}$  should be independent of the size of the system (apart for small  $n$ , for which the area law shows a transient). Regarding the presence of bound entanglement, we see in Fig. 1 that, e.g., for  $T=0.45$  the log negativity in the half-half partition is zero, meaning that single particles cannot distill, nevertheless, the system is entangled, as shown by the non-zero log negativity in the even-odd partition. For the reasons exposed in Sec. II we then conclude that for that temperature the system is bound entangled.

An exhaustive evidence of the presence of bound entanglement for any coupling constant is given in the  $T$ - $c$  diagram of Fig. 2. There we see that the threshold  $T_{\text{th}}^{e:o}$  is strictly larger than  $T_{\text{th}}^{h:h}$  for any  $c$ , indicating the existence of a bound entanglement region as soon as  $c \neq 0$ . The calculations are in this case performed for systems composed by 800 oscillators. The range of temperatures  $T_{\text{th}}^{h:h} < T < T_{\text{th}}^{e:o}$  for which bound entanglement is guaranteed is seen to increase when the system approaches the critical point  $c=0.5$ .

As said, the fact that all the half-half partitions are PPT implies that no entanglement can be distilled by means of local operations performed on each particle. However, it does not exclude the possibility that each oscillator is entangled with the others [26]. Interestingly, we also found a region of temperatures for which none of the oscillators is

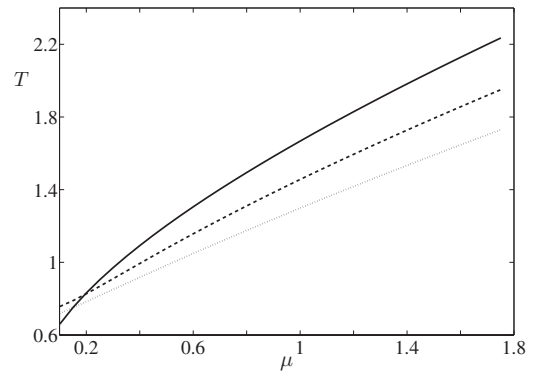


FIG. 3.  $T_{\text{th}}^{e:o}$  (solid line),  $T_{\text{th}}^{1:n-1}$  (dashed line), and  $T_{\text{th}}^{h:h}$  (dotted line) as a function of the coupling constant  $\mu$  for the Harmonic chain with next-nearest-neighbor interactions in Eq. (7) composed by 200 oscillators.

entangled with the rest of the chain, yet the global state is entangled (shaded region in Fig. 2). This is shown by calculating the log negativity for the partitions  $1:n-1$ , i.e., one particle vs the others. Since the partition consists of 1 vs  $n-1$  modes, the PPT condition turns out to be sufficient for separability [27]. We have calculated also the threshold temperatures corresponding to a generic contiguous splitting  $\frac{n}{2} - m : \frac{n}{2} + m$  (with  $0 \leq m \leq \frac{n}{2} - 1$ ). It can be seen that these threshold temperatures increase with  $m$ , that is, the entanglement in the bipartition  $1:n-1$  is the more robust to thermal noise among all these splittings.

In order to analyze the dependence of the results above on the system size, we have plotted the threshold temperatures as a function of  $n$  (see the inset of Fig. 2). In accordance to what was discussed, we see that the threshold temperatures remain constant. As a consequence, also the gap  $T_{\text{th}}^{e:o} - T_{\text{th}}^{h:h}$ , which determines the temperature range in which bound entanglement is present, is independent of the size of the system. These results strongly suggest that bound entanglement can also be observed in the macroscopic limit, an issue to which we will return in the next section.

Due to the generality of the area law, the results obtained for the nearest-neighbor model above are expected to be valid in a variety of different cases. As an example we report here the next-to-nearest interaction  $V^{\text{nn}}$  introduced in the previous subsection. In the  $T$ - $\mu$  diagram of Fig. 3 we can see that there is again a wide range of temperatures for which bound entanglement is present, as detected by the coexistence of nonzero log negativity in the even-odd partition and zero log negativity in the half-half one. Notice that the absence of an energy gap for  $\mu \leq 1$  does not affect qualitatively the presence of bound entanglement [28]. As said above, this can be related to the fact that an area law also holds for gapless systems in the case of nonzero temperatures.

### C. Analytical results

As pointed out in the previous section, the validity of a strict area law suggests both the independence of the threshold temperatures from the size of the system as well as the preservation of thermal bound entanglement for macroscopic

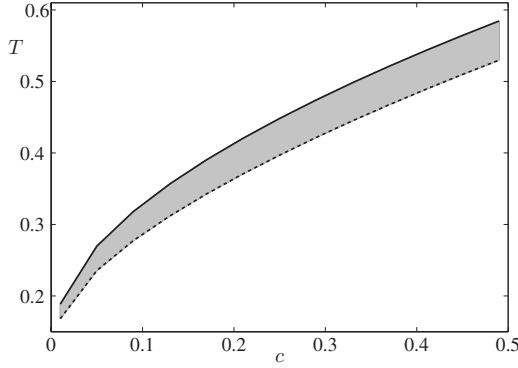


FIG. 4. The solid line represents  $T_{\text{th}}^{e:o}$  in the macroscopic limit, accordingly to Eq. (11): below this line the state of the system is entangled. The dashed line represents the upper bound to  $T_{\text{th}}^{h:h}$  as given by Eq. (31) (e.g., we considered  $m=10$  and  $s=3$ ): above this line the log negativity in the half-half partition is zero. In the shaded region then we can guarantee the presence of bound entanglement in the macroscopic limit.

systems. In this section we will analytically prove that this is actually the case. In particular, we will establish, for the paradigmatic system in Eq. (6), a formula for  $E_I$  in the even-odd partition and an upper bound for  $T_{\text{th}}^{h:h}$  in the half-half partition. Both will be obtained in the macroscopic limit, i.e., for  $n \rightarrow \infty$ . The remaining part of this section is quite technical. The reader not interested in the details can skip the proof, whose results are for convenience summarized in Fig. 4.

Let us start with the case of the even-odd partition, for which we can analytically prove the linear increase of the log negativity with the system size, as well as obtain the threshold temperature  $T_{\text{th}}^{e:o}$  as a function of the coupling  $c$ . The proof involves the calculation of the spectrum of  $Q$  in Eq. (5), and it follows closely the one given in Ref. [23] for the ground-state case. Consider the Hamiltonian (1) and a generic potential with translational invariance symmetry and periodic boundary conditions. Then,  $V$  is a circulant matrix and the matrices  $\omega^\pm$  can be diagonalized by a discrete Fourier transformation implemented by

$$\Omega_{k,l} = \exp\left(kl \frac{2\pi i}{n}\right) / \sqrt{n}, \quad (8)$$

with  $0 \leq k, l \leq n-1$ . Namely, one has that  $\Omega \omega^\pm \Omega^\dagger = D^\pm$  with  $D_{kl}^\pm = \delta_{kl} d_k^\pm$  and  $d_k^\pm = \Lambda_k^{\pm 1/2} \tanh(\sqrt{\Lambda_k}/2T)$  where  $\Lambda_k$  are the eigenvalues of  $V$ . Concerning the matrix  $P$ , one has that

$$\Omega P \Omega^\dagger = \tilde{P} = \begin{pmatrix} 0 & 1_{n/2} \\ 1_{n/2} & 0 \end{pmatrix}. \quad (9)$$

The spectrum of  $Q$  coincides then with the one of  $\tilde{P} D \tilde{P} D^\dagger$ , which in turn is straightforward to calculate due to its block diagonal structure. The eigenvalues of  $Q$  are hence given by  $d_k^- d_{k+n/2}^+$  and  $d_{k+n/2}^- d_k^+$ , for  $k=0, \dots, n/2-1$ . Specializing these results to the nearest-neighbor case in Eq. (6), one has that the eigenvalues of  $V^n$  are given by  $\Lambda_k = 1 - 2c \cos(2\pi k/n)$ . Defining the function

$$f(k, n, c, T) = \sqrt{\frac{\Lambda_{k+n/2}}{\Lambda_k}} \tanh\left(\frac{\sqrt{\Lambda_k}}{2T}\right) \tanh\left(\frac{\sqrt{\Lambda_{k+n/2}}}{2T}\right) \quad (10)$$

one has that the eigenvalues of  $Q$  that can contribute to the log negativity (i.e., that can be larger than one in dependence of the parameters) are given by  $f(k, n, c, T)$ , with double multiplicity and  $k=0, \dots, n/4$  (for  $n$  multiple of 4,  $n \geq 4$ ). The function  $f(k, n, c, T)$  is nonincreasing in  $k$  for the range of interest ( $0 \leq c < 1/2$  and  $T \geq 0$ ), and in particular it attains its maximum for  $k=0$ . As a consequence, the log negativity of the even-odd partition is different from zero when the temperature  $T$  is such that  $f(0, n, c, T) > 1$ , namely,

$$\sqrt{\frac{1+2c}{1-2c}} \tanh\left(\frac{\sqrt{1-2c}}{2T}\right) \tanh\left(\frac{\sqrt{1+2c}}{2T}\right) > 1. \quad (11)$$

In particular, the curve  $f(0, n, c, T) = 1$  gives the threshold temperature  $T_{\text{th}}^{e:o}$ . It coincides with the one depicted in Fig. 2 (solid line) and it is worth noticing that it does not depend on the total number of particles  $n$  (see also the solid line in the inset of Fig. 2), i.e., it holds also in the macroscopic limit. For temperatures below  $T_{\text{th}}^{e:o}$  there exists a  $\bar{k}(n, c, T)$  such that  $f(k, n, c, T) > 1$  for  $k < \bar{k}(n, c, T)$ , which in turn gives rise to the following expression for the log negativity:

$$E_I = \sum_{k=0}^{\bar{k}(n, c, T)} \log_2 \{f(k, n, c, T)\}. \quad (12)$$

Following again Ref. [23], we have that for large  $n$  the sum over  $k$  can be replaced by an integral over  $x = 2\pi k/n$ :

$$E_I = \frac{n}{2\pi} \int_0^{\bar{x}(c, T)} dx \log_2 \{f(x, c, T)\}. \quad (13)$$

Since  $f(k, n, c, T)$  in Eq. (10) actually depends only on the parameter  $x$ , we have that both the integrand and the upper bound  $\bar{x}(c, T)$  turn out to be independent of  $n$ . As a consequence the log negativity grows linearly with the system size in the macroscopic limit also for nonzero temperatures.

Regarding the half-half partition, we were not able to find an analytic expression for the log negativity in the macroscopic limit. Nevertheless, it is possible to find an exact upper bound for the threshold temperature  $T_{\text{th}}^{h:h}$ . As said, this allows us to identify an interval of temperatures for which the presence of bound entanglement can be guaranteed also in the macroscopic limit. We proceed as follows. Let us define the matrix

$$X_{ij} = \omega_{ij}^- \sum_{k=0}^{n/2-1} \sum_{h=n/2}^{n-1} (\delta_{ik} \delta_{jh} + \delta_{jk} \delta_{ih}), \quad (14)$$

where  $\delta_{ij}$  denotes the Kronecker delta. According to Ref. [18], the log negativity in the half-half partition is zero when the following inequality is satisfied:

$$\lambda_{\min}[W(T)]^{-2} + 2 \max_i |\lambda_i[X\omega^+]| < 1, \quad (15)$$

where the minimum eigenvalue of  $W(T)$  is given by

$$\lambda_{\min}[W(T)] = \frac{e^{\sqrt{1+2c/T} + 1}}{e^{\sqrt{1+2c/T} - 1}}. \quad (16)$$

Recognizing that the second term on the left hand side of Eq. (15) is twice the spectral radius  $r(X\omega^+)$  of the matrix  $X\omega^+$ , we can use any matrix norm to bound it from above [29]. In particular, let us consider the maximum row sum matrix norm  $\|\cdot\|_\infty$ , defined for a generic matrix  $A$  as

$$\|A\|_\infty \equiv \max_i \sum_j |A_{ij}| \quad (17)$$

(in what follows, we will omit the subscript for the sake of convenience). An upper bound for  $r(X\omega^+)$  is then given by  $r(X\omega^+) \leq \|X\omega^+\|$ , from which it follows that

$$r(X\omega^+) \leq \|X\|\|\omega^+\|. \quad (18)$$

Before proceeding in bounding  $\|X\|$  and  $\|\omega^+\|$ , let us write explicitly their elements in the macroscopic limit. Recall that  $\omega^\pm$  are circulant matrices, hence completely specified by their first row  $\omega^\pm = \mathcal{C}(v_0^\pm, \dots, v_{n-1}^\pm)$ , whose elements are in turn given by the discrete Fourier transform of the eigenvalues  $d_k^\pm$  introduced above:

$$v_l^\pm = \frac{1}{n} \sum_{k=0}^{n-1} d_k^\pm \exp\left(\frac{2\pi i}{n} kl\right). \quad (19)$$

In the limit  $n \rightarrow \infty$  the discrete sum above yields the Riemann sum for the following integral in the argument  $x = 2\pi k/n$ :

$$v_l^\pm = \frac{1}{2\pi} \int_0^{2\pi} dx d^\pm(x) e^{ixl}, \quad (20)$$

that is,  $v_l^\pm$  are the Fourier coefficients of the periodic functions  $d^\pm(x)$ :

$$d^\pm(x) = (1 - 2c \cos x)^{\pm 1/2} \tanh\left(\frac{\sqrt{1 - 2c \cos x}}{2T}\right). \quad (21)$$

Notice that  $d^\pm(x)$  are smooth functions, which implies an exponential decay of  $|v_l^\pm|$  as a function of  $l$ . In fact, for any integer  $s$ , by integrating by parts  $s$  times we have

$$|v_l^\pm| = \frac{1}{2\pi} \left| \frac{1}{(il)^s} \int_0^{2\pi} dx e^{ixl} \frac{d}{dx^s} d^\pm(x) \right| \leq \frac{1}{2\pi} \frac{1}{l^s} C_s^\pm, \quad (22)$$

where  $C_s^\pm \equiv \int_0^{2\pi} dx |d_{dx^s}^\pm(x)|$ . Let us now bound first  $\|\omega^+\|$ . Being  $\omega^+$  a circulant matrix, there is no need to look for the maximum in Eq. (17), as the rows are composed by the same elements. Then one can write, for any integer  $m$ ,  $\|\omega^+\| = S_m^+ + \mathcal{E}_m^+$ , where we defined the partial sum and the residual term, respectively, as follows:

$$S_m^+ \equiv \sum_{l=-m}^m |v_l^+|, \quad \mathcal{E}_m^+ \equiv 2 \sum_{l=m+1}^\infty |v_l^+|. \quad (23)$$

In order to obtain a bound on  $\|\omega^+\|$  one can now fix  $m$ , calculate explicitly  $S_m^+$ , and bound  $\mathcal{E}_m^+$  from above. This latter step can be achieved by exploiting again the property of  $d^\pm(x)$  and integrating by parts  $s$  times, leading to

$$\mathcal{E}_m^+ \leq \frac{C_s^+}{\pi} \zeta(s, m+1), \quad (24)$$

where  $\zeta(s, m+1)$  is the generalized Riemann zeta function. Summarizing, one has that for any integer  $s$  and  $m$

$$\|\omega^+\| \leq S_m^+ + \frac{C_s^+}{\pi} \zeta(s, m+1), \quad (25)$$

the bound becoming tighter for large  $m$  and  $s$ .

Let us now determine an upper bound for  $\|X\|$ . First, for any finite  $n$ , the matrix  $X$  has a bipartite symmetric structure of the following form:

$$X = \begin{pmatrix} 0 & B \\ B & 0 \end{pmatrix},$$

where  $B$  is a  $\frac{n}{2} \times \frac{n}{2}$  symmetric Toeplitz matrix. Then  $\|X\|$  coincides with  $\|B\|$  and in order to evaluate the latter we need to determine which row of  $B$  gives rise to the maximum in Eq. (17). Fortunately, in the macroscopic limit  $n \rightarrow \infty$  the periodic boundary conditions can be disregarded and the last row of  $B$  determines its norm. This is because going from the last to the next to the last row we simply remove the term  $|v_1^-|$  from the sum in Eq. (17), and so on for the other rows. It can be seen that this is the case also taking rigorously into account the periodic boundary conditions. By writing explicitly matrix  $B$ ,

$$B = \begin{pmatrix} v_{n/2}^- & v_{n/2-1}^- & \dots & v_2^- & v_1^- \\ v_{n/2-1}^- & \ddots & \ddots & & v_2^- \\ \vdots & \ddots & \ddots & \ddots & \vdots \\ v_2^- & & \ddots & \ddots & v_{n/2-1}^- \\ v_1^- & v_2^- & \dots & v_{n/2-1}^- & v_{n/2}^- \end{pmatrix},$$

and exploiting its symmetries, we see that our considerations can be restricted to the last  $n/4$  rows (or, equivalently, to the first  $n/4$  rows). Define for a generic row the following sum ( $j=1, \dots, n/4$  denotes the rows in reverse order, from the last to the  $\frac{n}{4}$ th one):

$$R_j = \sum_{l=j}^{n/2-1} |v_l^-| + \sum_{l=(n/2)+1-j}^{n/2} |v_l^-|, \quad (26)$$

such that  $\|B\| = \max_j R_j$ . The difference between  $R_j$  for a generic row and  $R_1$  can be bound from above as follows:

$$R_j - R_1 = \sum_{l=(n/2)+1-j}^{n/2} |v_l^-| - \sum_{l=1}^j |v_l^-| \leq \sum_{l=(n/2)+1-j}^{n/2} |v_l^-|, \quad (27)$$

which implies that

$$\max_j (R_j - R_1) \leq \sum_{l=(n/4)+1}^{n/2} |v_l^-|. \quad (28)$$

Since the sum above goes to zero for  $n \rightarrow \infty$  [as can be explicitly seen by exploiting the exponential decay of  $|v_l^-|$  in Eq. (22)], we have that the error made by considering the last row of  $B$  as the one that gives the maximum in evaluating

$\|B\|$  can be made as small as one may wish. In other words, we can identify  $\|X\|=R_1$ .

Now, we can proceed as we did for  $\|\omega^+\|$ . In particular defining again the partial sum as

$$S_m^- \equiv \sum_{l=1}^m |v_l^-|, \quad (29)$$

we obtain that for any integer  $s$  and  $m$

$$\|X\| \leq S_m^- + \frac{C_s^-}{2\pi} \zeta(s, m+1), \quad (30)$$

where again  $S_m^-$  can be calculated explicitly and the bound becomes tighter for large  $m$  and  $s$ .

Summarizing, considering Eqs. (15), (16), (25), and (30), we have shown that, in the macroscopic limit, the log negativity in the half-half partition is zero when the following inequality is satisfied:

$$2 \left( S_m^+ + \frac{C_s^+}{\pi} \zeta(s, m+1) \right) \left( S_m^- + \frac{C_s^-}{2\pi} \zeta(s, m+1) \right) + \left( \frac{e^{\sqrt{1+2c/T}} - 1}{e^{\sqrt{1+2c/T}} + 1} \right)^2 < 1. \quad (31)$$

Based on the formula above and on Eq. (11), we depicted in Fig. 4 the region in the  $c$ - $T$  plane for which bound entanglement is present in the macroscopic limit (shaded region). We see that for any coupling  $c$  we can guarantee that there is an interval of temperatures for which the negativity in the half-half partition is zero, nevertheless, the state is entangled.

Finally, let us mention an issue concerning the procedure used in order to derive Eq. (11). We considered a finite system composed by  $n$  particles and calculated explicitly  $T_{\text{th}}^{e:o}$ . We have seen that it does not depend on  $n$  and so argued that it has to be valid also in the limit  $n \rightarrow \infty$ . On the other hand, one could have considered first the limit  $n \rightarrow \infty$  and then analyzed a distinguished region of the system for increasing size [as we did in deriving Eq. (31)]. The two procedures are equivalent, since no convergence problem appears in the spectrum of  $V^m$  for  $n \rightarrow \infty$ .

#### IV. SPIN SYSTEMS

As already mentioned, we go beyond the harmonic oscillator case and also investigate the existence of bound entangled thermal states in spin systems. Consider the Hamiltonian

$$H_{XX} = -J \sum_{i=1}^n (\sigma_i^x \sigma_{i+1}^x + \sigma_i^y \sigma_{i+1}^y) + B \sum_i \sigma_i^z, \quad (32)$$

that is,  $n$  spin  $\frac{1}{2}$  particles with nearest-neighbor  $XX$  interactions with coupling constant  $J$  and subject to a transverse magnetic field  $B$ . For this system we also calculate the thermal-state entanglement, measured now by the negativity  $E_N$ , for different partitions. All the obtained results are consistent with the previous reasoning: there is a temperature range for which the negativity in the half-half partitions is

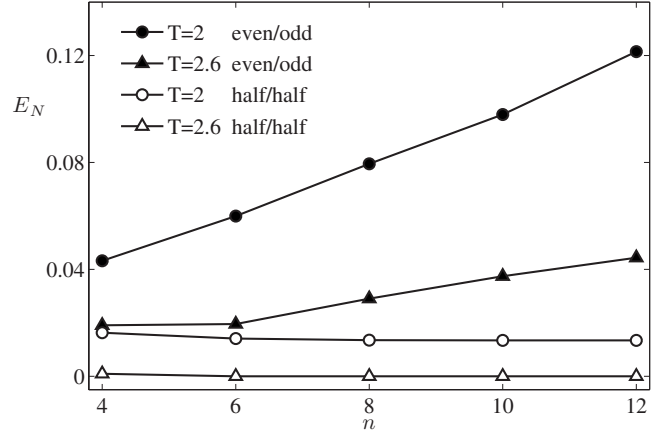


FIG. 5. Negativity in the even-odd (full symbols) and half-half (empty symbols) partitions for the thermal states of the Hamiltonian (32) with  $B=1.9$  and  $J=1$ . The temperatures for each partition are set to be  $T=2$  and  $2.6$  (see legend). In the even-odd partition we can clearly see an increase of the negativity with respect to the system size, whereas it saturates in the half-half partition. For  $T=2.6$  we see that the state is bound entangled (the negativity in the half-half partition being zero).

zero, nevertheless, the system is still entangled as proven by the negativity in the even-odd partition. Although in this case we are not able to deal with big systems, our results suggest an entanglement area law for nonzero temperature and the independence of the gap  $T_{\text{th}}^{e:o} - T_{\text{th}}^{h:h}$  with the system size, as found in the harmonic oscillator case.

In Fig. 5 we plot the negativity for the even-odd (full symbols) and for the half-half (empty symbols) partitions, for two different values of the temperature. For a constant number of bonds between the partitions as in the case of the half-half splitting the negativity does not depend on the system size  $n$ , whereas for the even-odd partition it increases with  $n$ . This behavior resembles the previous study for harmonic oscillators (see Fig. 1), and the same reasonings apply here to show the presence of bound entanglement.

In order to study the PPT condition in a system with  $n=10$  particles for different values of the coupling constant  $J$ , we plot the corresponding separability temperature in Fig. 6 for three different bipartite splittings. In all the range of values of  $J$  the separability temperature corresponding to the even-odd partition  $T_{\text{th}}^{e:o}$  is strictly higher than  $T_{\text{th}}^{1:n-1}$  and  $T_{\text{th}}^{h:h}$ , corresponding to the  $1:n-1$  and half-half partitions, respectively. The corresponding threshold temperatures for PPT are shown in the inset of Fig. 6 for increasing system sizes. For  $n > 6$  the gap between these temperatures appears constant (we only compute these values for systems with an even number of particles for symmetry reasons).

We can tune the local field  $B$  of the Hamiltonian Eq. (32) in such a way that the system ground state exhibits some interesting entanglement properties. For a local field  $B=1.9$  and  $J=1$  the ground state of the system is a generalized  $W$  state of  $n$  spins [30], whereas for  $B > 2$  the ground state is the product state  $|00 \cdots 0\rangle$ . In Fig. 7 we plot, for different values of the field  $B$  and  $T=0.1$ , the negativity for the even-odd and half-half partitions. Notice the presence of the characteristic dips due to the mixing of different entangled ground states

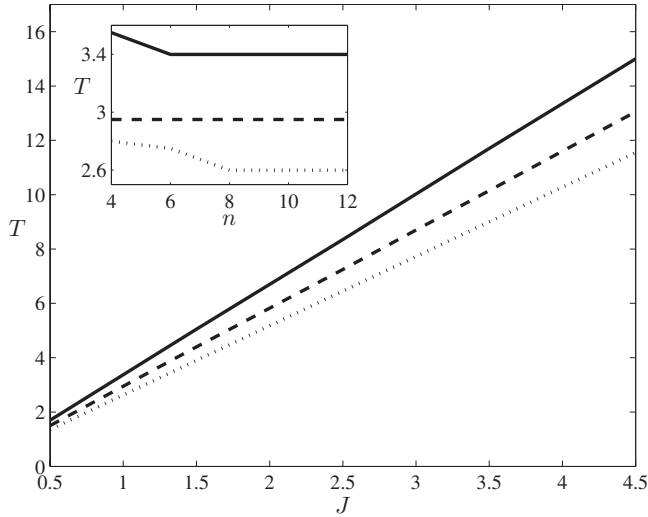


FIG. 6. Threshold temperatures above which the negativity is zero in the even-odd ( $T_{\text{th}}^{e:o}$ , solid line),  $1:n-1$  ( $T_{\text{th}}^{1:n-1}$ , dotted line), and half-half ( $T_{\text{th}}^{h:h}$ , dashed line) partitions. We plot the threshold temperature as a function of the coupling parameter  $J$  of the Hamiltonian (32) with  $n=10$  and  $B=1.9$ . Inset: Temperature above which the negativity in the even-odd ( $T_{\text{th}}^{e:o}$ , solid line),  $1:n-1$  ( $T_{\text{th}}^{1:n-1}$ , dotted line), and half-half ( $T_{\text{th}}^{h:h}$ , dashed line) partitions is zero as a function of the number  $n$  of spins with Hamiltonian (32) with  $J=1$  and  $B=1.9$ .

[31]. In particular, we can see that for  $B < 2$  the even-odd partition has a higher degree of entanglement than the half-half partition. As a consequence, the main points of our intuition for the emergence of bound entanglement are still valid, also in the presence of complex behaviors like the ones shown in Fig. 7.

For low temperatures and values of the local field  $B > 2$  the ground state (separable) dominates the system and therefore the thermal state is separable for all the partitions. For higher temperatures the state turns out to be a combination of

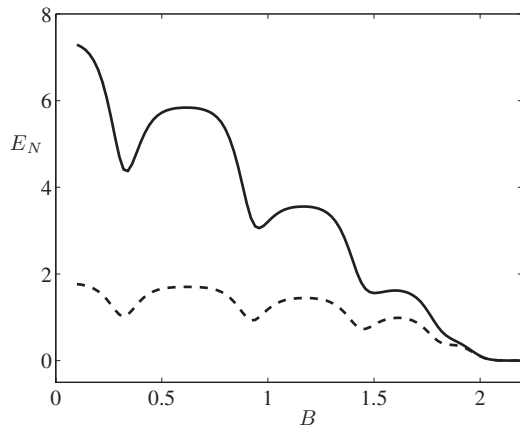


FIG. 7. Negativity in the even-odd (solid line) and half-half (dashed line) partitions for the thermal states of Hamiltonian (32) with  $n=10$ ,  $J=1$ , and  $T=0.1$  as a function of  $B$ . For  $B > 2$  the ground state is the separable state  $|00 \cdots 0\rangle$ , but some amount of entanglement still appears due to the mixture with entangled excited states.

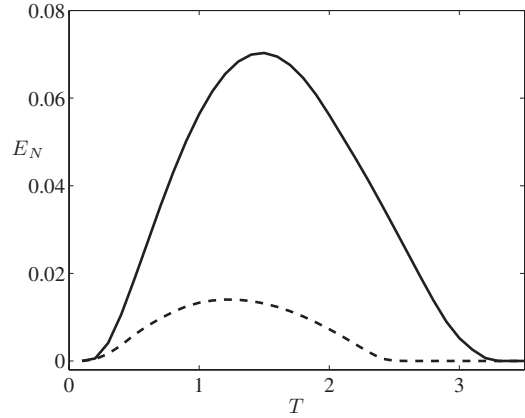


FIG. 8. Negativity in the even-odd (solid line) and half-half (dashed line) partitions for  $n=10$ ,  $J=1$ , and  $B=2.3$  for spin  $\frac{1}{2}$  particles with Hamiltonian (32). As expected, the negativity in the even-odd partition is greater than the corresponding to the half-half partition, and bound entanglement appears in the temperature range  $2.5 < T < 3.2$ .

the separable ground state and some excited states that can be entangled [32]. In this condition entanglement can be increased by raising the temperature. This is shown in Fig. 8, where we plot the negativity for fixed field  $B=2.3$  as a function of the temperature for the even-odd and half-half partitions. We can see again that the negativity in the even-odd partition is higher than the respective values for the half-half partition. In particular, in the range  $2.5 < T < 3.2$  the half-half partition is PPT while the negativity in the even-odd partition is non-null. Thus also in these quite peculiar conditions—in which the ground state has  $E_N=0$ —we see, for increasing temperatures, that (i) when the system becomes entangled (i.e., for small  $T$  greater than zero) the negativity is higher in the even-odd partition and (ii) before the system becomes separable (i.e., for higher  $T$ ) it passes through a nondistillable region. This behavior again supports the general validity of our considerations.

Finally, we mention that we have found an analogous behavior in systems subjected to the Heisenberg interaction,

$$H_{XXX} = \sum_{i=1}^n (\sigma_i^x \sigma_{i+1}^x + \sigma_i^y \sigma_{i+1}^y + \sigma_i^z \sigma_{i+1}^z) + B \sum_i \sigma_i^z, \quad (33)$$

for which a study of the entanglement properties of two neighboring spins was shown in [31]. In this model a value of the local field  $B > 4$  produces the ground state  $|00 \cdots 0\rangle$ . From this point the results and considerations for this model are essentially equivalent to those corresponding to the XX model.

### V. CONCLUDING REMARKS

In closing this paper, we point out a few remarks regarding the obtained results. First, we have shown the existence of thermal bound entanglement by considering local ( $n$ -party) distillation strategies. One can also pose the question whether fully PPT entanglement can exist in these systems, that is, entangled states such that all bipartite partitions

are PPT. Actually, as shown in Ref. [8], fully PPT entanglement can be found for spin systems, at least up to nine qubits. On the other hand, our results, when combined with those of Refs. [33,34], prove that fully PPT entangled states cannot be obtained for the harmonic systems studied here. In Ref. [33] bounds are derived for the threshold temperatures for full separability of various harmonic systems. Remarkably, these upper bounds are tight in the case of systems with sufficient translational symmetries, as in the case of the nearest-neighbor interaction in Eq. (6). It is then possible to depict a kind of phase diagram in the  $T$ - $c$  plane separating two regions, one in which the state is separable and the other in which quantum correlations are present in some form. Such a threshold turns out to coincide with the one given by Eq. (11) for the zero negativity in the even-odd partition. Thus the thermal states of this system become PPT and fully separable for the same temperature. We mention here that such a result holds also for other systems, for example, for the one given in Eq. (7). However, in these cases we had to approach the problem numerically (based on the results of Ref. [34]) and consider only finite systems.

Finally, let us stress that our results enrich the above mentioned phase diagram of Ref. [33], in the sense that we can distinguish a third region in it where quantum correlations are present but they are not distillable. In particular, referring to Figs. 2 and 4, we have that, by rising the temperature at fixed coupling, the system goes from a genuinely entangled state (in which all the bipartitions are NPPT) to a bound

entangled state and finally becomes just classically correlated. As already discussed, we have found that such a behavior is common to all the harmonic systems we took in consideration. For spin systems, a similar phase diagram holds, at least for the finite-size systems studied here.

In conclusion, we have shown the existence of thermal-state bound entanglement for several quantum many-body systems. We explicitly considered systems composed by hundreds of oscillators and observed in general an area law for thermal states. These findings turned out to be crucial in proving the existence of bound entanglement also in the macroscopic limit for harmonic systems. As a consequence, and by virtue of the generality of area laws, these results have been shown to be valid for a variety of other systems, as well as in the presence of complex behaviors of the entanglement. All these considerations strongly support the existence of thermal-state bound entanglement in the macroscopic limit also for finite-dimensional systems.

#### ACKNOWLEDGMENTS

We thank S. M. Giampaolo, F. Illuminati, G. Tóth, and M. O. Terra Cunha for helpful comments. This work was supported by the EU QAP project, the Spanish MEC, under Grant No. FIS2007-60182 and Consolider-Ingenio QOIT projects, and a “Juan de la Cierva” grant, the Generalitat de Catalunya, and the Università di Milano under grant “Borse di perfezionamento all’estero.”

- 
- [1] C. H. Bennett, G. Brassard, S. Popescu, B. Schumacher, J. A. Smolin, and W. K. Wootters, *Phys. Rev. Lett.* **76**, 722 (1996).
- [2] C. H. Bennett, D. P. DiVincenzo, J. A. Smolin, and W. K. Wootters, *Phys. Rev. A* **54**, 3824 (1996).
- [3] M. Horodecki, P. Horodecki, and R. Horodecki, *Phys. Rev. Lett.* **80**, 5239 (1998).
- [4] Given a bipartite state  $\rho$ , its partial transposition, say with respect to the first subsystem, is equal to  $\rho^{T_1} = \sum_{ijkl} \rho_{ijkl} |jk\rangle\langle il|$ , where  $\rho_{ijkl} = \langle ik|\rho|jl\rangle$ . As shown in A. Peres, *Phys. Rev. Lett.* **77**, 1413 (1996), if  $\rho$  is separable, its partial transposition is a positive operator.
- [5] P. Horodecki, *Phys. Lett. A* **232**, 333 (1997).
- [6] W. Dür, J. I. Cirac, M. Lewenstein, and D. Bruß, *Phys. Rev. A* **61**, 062313 (2000); D. P. DiVincenzo, P. W. Shor, J. A. Smolin, B. M. Terhal, and A. V. Thapliyal, *ibid.* **61**, 062312 (2000).
- [7] For a review, see R. Horodecki, P. Horodecki, M. Horodecki, and K. Horodecki, e-print arXiv:quant-ph/0702225.
- [8] G. Tóth, C. Knapp, O. Gühne, and H. J. Briegel, *Phys. Rev. Lett.* **99**, 250405 (2007).
- [9] D. Patané, R. Fazio, and L. Amico, *New J. Phys.* **9**, 322 (2007).
- [10] A. Ferraro, D. Cavalcanti, A. Garcia-Saez, and A. Acín, *Phys. Rev. Lett.* **100**, 080502 (2008).
- [11] L. Amico, R. Fazio, A. Osterloh, and V. Vedral, *Rev. Mod. Phys.* **80**, 517 (2008).
- [12] T. J. Osborne and M. A. Nielsen, *Phys. Rev. A* **66**, 032110 (2002); A. Osterloh, L. Amico, G. Falci, and R. Fazio, *Nature* (London) **416**, 608 (2002); G. Vidal, J. I. Latorre, E. Rico, and A. Kitaev, *Phys. Rev. Lett.* **90**, 227902 (2003).
- [13] C. H. Bennett, H. J. Bernstein, S. Popescu, and B. Schumacher, *Phys. Rev. A* **53**, 2046 (1996).
- [14] S. Popescu and D. Rohrlich, *Phys. Rev. A* **56**, R3319 (1997).
- [15] L. Bombelli, R. K. Koul, J. H. Lee, and R. D. Sorkin, *Phys. Rev. D* **34**, 373 (1986); M. Srednicki, *Phys. Rev. Lett.* **71**, 666 (1993).
- [16] M. B. Plenio, J. Eisert, J. Dreißig, and M. Cramer, *Phys. Rev. Lett.* **94**, 060503 (2005).
- [17] R. G. Unanyan and M. Fleischhauer, *Phys. Rev. Lett.* **95**, 260604 (2005).
- [18] M. Cramer, J. Eisert, M. B. Plenio, and J. Dreißig, *Phys. Rev. A* **73**, 012309 (2006).
- [19] G. Vidal and R. F. Werner, *Phys. Rev. A* **65**, 032314 (2002).
- [20] M. M. Wolf, F. Verstraete, M. B. Hastings, and J. I. Cirac, *Phys. Rev. Lett.* **100**, 070502 (2008).
- [21] In fact, due to the translational invariance of the systems considered here, all the half-half partitions are equivalent.
- [22] We have set to 1 the mass and the proper frequencies of the oscillators (see, e.g., Ref. [11]), whereas the parameters in  $V$  are taken dimensionless. Besides, quantities are made dimensionless throughout the paper whenever necessary.
- [23] K. Audenaert, J. Eisert, M. B. Plenio, and R. F. Werner, *Phys. Rev. A* **66**, 042327 (2002).
- [24] A. Botero and B. Reznik, *Phys. Rev. A* **70**, 052329 (2004).
- [25] N. Schuch, J. I. Cirac and M. M. Wolf, *Commun. Math. Phys.*

- 267**, 65 (2006).
- [26] J. A. Smolin, Phys. Rev. A **63**, 032306 (2001).
- [27] R. F. Werner and M. M. Wolf, Phys. Rev. Lett. **86**, 3658 (2001).
- [28] Notice that the details of the model (in particular, the peculiar independence of the coupling between next-nearest neighbors on  $\mu$ ) implies that for small  $\mu$  the negativity is higher in the contiguous partitions than in the even-odd one.
- [29] R. A. Horn and C. R. Johnson, *Matrix Analysis* (Cambridge University Press, Cambridge, U.K., 1985).
- [30] D. Bruß, N. Datta, A. Ekert, L. C. Kwek, and C. Macchiavello, Phys. Rev. A **72**, 014301 (2005).
- [31] M. C. Arnesen, S. Bose, and V. Vedral, Phys. Rev. Lett. **87**, 017901 (2001).
- [32] D. W. Berry and M. R. Dowling, Phys. Rev. A **74**, 062301 (2006).
- [33] J. Anders and A. Winter, Quantum Inf. Comput. **8**, 245 (2008).
- [34] P. Hyllus and J. Eisert, New J. Phys. **8**, 51 (2006).